Journal of Biomolecular NMR, **16:** 109–119, 2000.
KLUWER/ESCOM

Peptide self-association in aqueous trifluoroethanol monitored by pulsed field gradient NMR diffusion measurements

Shenggen Yao[a,*], Geoffrey J. Howlett[b] & Raymond S. Norton[a,**]
[a]*Biomolecular Research Institute, 343 Royal Parade, Parkville, VIC 3052, Australia*
[b]*Department of Biochemistry and Molecular Biology, University of Melbourne, Parkville, VIC 3052, Australia*

Received 19 August 1999; Accepted 30 November 1999

Key words: apparent molecular mass, internal standard, neuropeptide Y, pulsed field gradient NMR, self-association, translational self-diffusion coefficient

Abstract

Defining the self-association state of a molecule in solution can be an important step in NMR-based structure determination. This is particularly true of peptides, where there can be a relatively small number of long-range interactions and misinterpretation of an intermolecular NOE as an intramolecular contact can have a dramatic influence on the final calculated structure. In this paper, we have investigated the use of translational self-diffusion coefficient measurements to detect self-association in aqueous trifluoroethanol of three peptides which are analogues of the C-terminal region of human neuropeptide Y. Experimentally measured diffusion coefficients were extrapolated to D^0, the limiting value as the peptide concentration approaches zero, and then converted to $D_{20,w}$, the diffusion coefficient after correction for temperature and the viscosity of the solvent. A decrease in $D_{20,w}$ of about 16% was found for all three peptides in aqueous TFE (30% by volume) compared with water, which is in reasonable agreement with the expected decrease upon dimerisation, the presence of which was indicated by sedimentation equilibrium measurements. Apparent molecular masses of these peptides in both solutions were also calculated from their diffusion coefficients and similar results were obtained. Several potential internal standards, including acetone, acetonitrile, dimethylsulfoxide and dioxane, were assessed as monitors of solution viscosity over a range of trifluoroethanol concentrations. Compared with independent measurements of viscosity, acetonitrile was the most accurate standard among these four. The practical limitations of a quantitative assessment of peptide self-association from translational diffusion coefficients measured by PFGNMR, including the calculation of apparent molecular mass, are also discussed.

Abbreviations: PFGNMR, pulsed field gradient NMR; NPY, neuropeptide Y; TFE, trifluoroethanol.

Introduction

Translational self-diffusion coefficients of proteins as measured by pulsed field gradient NMR have been used successfully for the characterisation of self-association and folding/unfolding processes in solution (Altieri et al., 1995; Dingley et al., 1995; Jones et al., 1997; Pan et al., 1997). Unlike traditional methods for monitoring biomolecular self-association, such as analytical ultracentrifugation or dynamic light scattering, the PFGNMR method allows the translation diffusion coefficient of the molecule to be determined under identical conditions to those used for determination of the solution structure. The state of self-association of a protein can be obtained directly from its diffusion coefficient or via the relationship between its mass and diffusion coefficient.

In practice, how directly an assessment of molecular self-association can be obtained from measure-

*Current address: Howard Florey Institute of Experimental Physiology and Medicine, University of Melbourne, Melbourne, VIC 3010, Australia.
**To whom correspondence should be addressed. E-mail: ray.norton@bioresi.com.au

ments of molecular translational self-diffusion coefficients by PFGNMR depends on whether a computation of the molecular mass is required. Altieri et al. (1995) showed that oligomerisation could be detected directly from diffusion constants without calculating molecular masses by comparing the measured diffusion coefficients with values for known monomeric proteins. Similarly, Dingley et al. (1995) were able to determine the concentration of detergent necessary to inhibit self-association of myosin light chain 2 by monitoring the protein's translational diffusion coefficient. Diffusion measurements have also been used to monitor lysozyme unfolding in urea, where a 38% increase in the effective hydrodynamic radius was inferred (Jones et al., 1997), and to characterise partially folded forms of bovine pancreatic trypsin inhibitor (Pan et al., 1997). In a different vein, changes in the diffusion coefficients of small molecules when bound to proteins can be used to identify protein ligands from complex mixtures of synthetic or naturally occurring chemicals emanating from screening programs (Lin et al., 1997; Chen et al., 1998).

In most of these applications the actual molecular mass corresponding to a given diffusion coefficient was not critical, the emphasis being on changes in structure or state of aggregation. In the work presented in this paper, we wished to determine the degree of self-association of a series of peptides in water and aqueous trifluoroethanol in parallel with studies of their solution structures and the design of new analogues. For the assessment of molecular self-association from translational diffusion coefficients in two different solvents, several approaches are possible, including (i) correcting the measured diffusion coefficients for temperature and solvent viscosity and extrapolating to zero solute concentration, (ii) introducing a small organic molecule as an internal standard against which measured diffusion coefficients are compared, and (iii) calculating the apparent molecular mass directly from the measured diffusion coefficients. In the present work, all three methods have been investigated, and the results are compared with those from sedimentation equilibrium measurements conducted on the same samples.

The peptides investigated in this work are related to the C-terminal region of neuropeptide Y (NPY). NPY is a 36-residue, C-terminally amidated, polypeptide hormone and neurotransmitter, active in both the central and peripheral nervous systems. It participates in the regulation of many physiological processes, including food intake, blood pressure, circadian rhythms, anxiety and sexual behaviour, these activities being mediated by at least six receptor subtypes (Y1–Y6) (Grundemar and Håkanson, 1994; Grundemar, 1997). The 13-residue C-terminal analogue Ac[Leu^{28,31}]NPY$^{24-36}$ is a potent and selective agonist for the Y2 receptor (Barden et al., 1994; Potter et al., 1994). It adopts a well-defined helical structure in aqueous trifluoroethanol (Barden et al., 1994; Barnham et al., 1999) and associates to form trimers or tetramers in this solvent (Barnham et al., 1999). The peptides examined here are analogues of this peptide that incorporate lactam bridges with the aim of stabilising the helical structure (Houston et al., 1995; Rist et al., 1996; Kirby et al., 1997); their amino acid sequences are shown in Figure 1.

Structural studies on these peptides, to be reported elsewhere, have shown that all three adopt helical structures in aqueous TFE, whereas in water only the lactam bridge region retains a helical–like turn structure. Representative structures of peptide **I** in water and in aqueous TFE are shown in Figure 2. As the parent peptide for this series, Ac[Leu^{28,31}]NPY$^{24-36}$, associates to form trimers or tetramers in aqueous TFE (Barnham et al., 1999), we were interested in determining if the lactam-bridge peptides showed similar behaviour. We have therefore measured their diffusion coefficients by PFGNMR in both water and aqueous TFE. Several ways of interpreting these data in terms of apparent molecular masses of the peptides have been explored and the results are compared with masses obtained from sedimentation equilibrium experiments.

Materials and methods

Sample preparation

All peptides used in the present study were obtained from AusPep (Melbourne, Australia). NMR samples were prepared by dissolving 2.8–4.8 mg of each peptide in 600 μl of H_2O containing 10% ^2H_2O by volume or 600 μl of H_2O containing 30% TFE-$^2H_3$ by volume. Concentration-dependence studies were carried out by adding a weighed amount of peptide to a diluted sample. The pH was adjusted to 5.0 by addition of small amounts of HCl or NaOH, and measured at 20 °C without correction for isotope or solvent effects. Samples used for the assessment of small organic molecules as potential internal standards in the presence of trifluoroethanol were prepared by adding 0.05 μl dioxane, acetone, acetonitrile

	24 36
hNPY	.....LRHYINLITRQRY-NH_2
Ac-cyclic$^{28/32}$ [Ala^{24} Lys^{28} Leu^{31} Glu^{32}] NPY$^{24-36}$ (I)	Ac-ARHYKNLLERQRY-NH_2
Ac-cyclic$^{28/32}$ [Ala^{24} Lys^{28} Glu^{32}] NPY$^{24-36}$ (II)	Ac-ARHYKNLIERQRY-NH_2
Ac-cyclic$^{28/32}$ [Lys^{28} Glu^{32}] NPY$^{25-36}$ (III)	Ac- RHYKNLIERQRY-NH_2

Figure 1. Amino acid sequences of peptides **I–III** used in the present study. All three peptides are analogues of the C-terminal region of human NPY, the amino acid sequence of which is shown at the top. The NPY numbering is used throughout this paper. The line between K28 and E32 represents a lactam bridge.

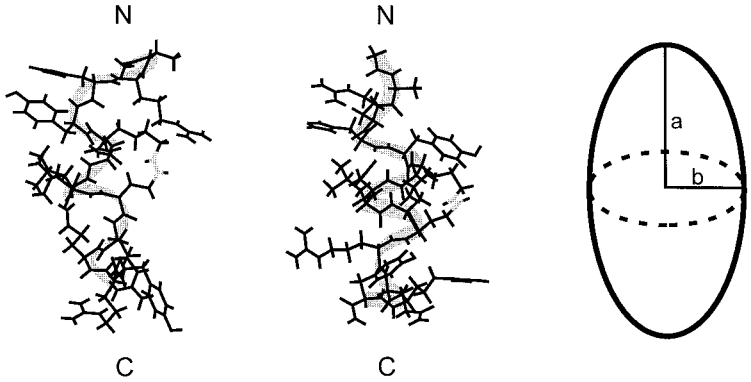

Figure 2. NMR-derived structures of peptide **I** in 90% H_2O/10% ^2H_2O (left) and 40% TFE-$^2H_3$/ 60% H_2O (middle) at 25 °C and pH 5.0 (Yao et al., to be published) and a schematic diagram of a prolate ellipsoid model used in estimating the shape-factor (right). The lactam bridges in both structures are on the right-hand side of the structures in grey. No substantial chemical shift differences were observed for those peptides between 20 and 25 °C or for volume fractions of TFE-$^2H_3$ in the range 30–40%.

and dimethylsulfoxide to 600 μl of H_2O containing different percentages by volume of TFE-$^2H_3$.

PFGNMR spectroscopy

PFGNMR spectra were acquired at 20 °C on a Bruker AMX-500 spectrometer using a 5 mm triple resonance probe with a single gradient (Z). A PFG longitudinal eddy-current delay (LED) pulse sequence incorporating crusher gradients during both longitudinal storage periods was used (Gibbs and Johnson, 1991; Dingley et al., 1995). Diffusion coefficients were measured by incrementing either the duration of the field gradient pulses (typically, with an initial value of 0.2 ms, a step size of 1.5 ms and magnitude ∼15.4 G cm^{-1}) or the amplitude (typically, with an initial value of ∼2.6 G cm^{-1} and a step size of 2.6 G cm^{-1} for 5 ms), while the separations (50 ms) of the field gradients and the total echo time were kept constant. A series of 12 spectra with 32, 64 or 128 scans was recorded in 2D mode for each measurement, with a recycle time of 6 s between scans. To ensure that equilibrium had been established with respect to sample temperature and molecular self-association processes, measurements were taken consecutively until no systematic change to the diffusion coefficients of the molecules was apparent.

Calibration of B_0 field gradient strength

The strength of the B_0 field gradient was calibrated firstly by measuring the self-diffusion coefficient of the residual H^2HO in a 100% ^2H_2O sample at 25 °C (Callaghan et al., 1983). A diffusion coefficient of 1.90×10^{-9} m^2 s^{-1} for that residual H^2HO signal (Longsworth et al., 1960) was used for back calculation of the gradient strength, in which both peak intensities (without manipulating the window function) and volumes were fitted to a single exponential decay. The strength of the B_0 field gradient was also

calibrated using a 4.0 mm high sample of 100% ^2H_2O in a Shigemi NMR tube. Both gradient-echo and spin-echo sequences were used to generate a spatial profile of the sample with the field gradient on during acquisition. A sufficient time delay was employed between the dephasing and rephasing gradient pulses to ensure that the dephasing gradient pulse had decayed completely before the rephasing gradient was turned on. Slightly higher values of Gz (3–5% for Gz up to 50 G cm^{-1}) were obtained with the first method by fitting the volumes, whereas the values of Gz from the first method by fitting the intensities without manipulating the window function were in very good agreement with those from the second method. Values of the strengths of the B_0 field gradient used in the present study were the average of those from the first method using peak intensities and the second method.

Translational diffusion induced signal attenuation and data processing

For a single diffusing species, the signal attenuation in the presence of a single pair of pulsed field gradients is given by

$$I = I_0 \exp(-\gamma^2 g^2 D \delta^2 (\Delta - \delta/3)) \quad (1)$$

where γ is the gyromagnetic ratio and g, δ and Δ are the amplitude, duration and separation of the single pair of gradient pulses, respectively (Stejskal and Tanner, 1965). All spectra were processed using XWINNMR 2.1 (Bruker). An exponential window function with 3 Hz line broadening was applied before the Fourier transformation (FT) and a baseline correction was then conducted after the FT. Data analyses were accomplished using the *relaxation* T_1/T_2 routine (Bruker). Diffusion constants were obtained by fitting peak intensities to a single exponential decay (Equation 1) using the program *Simfit* (Bruker). For each measurement, a number of peaks across the spectrum was used in the fitting and the average value was reported. No significant difference was observed by fitting peak intensities compared with peak volumes.

Analytical ultracentrifugation

Sedimentation experiments were performed using a Beckman XLA ultracentrifuge and Ti60 rotor. A 12 mm centrepiece and a sample volume of 100 μl were used in all measurements. Measurements on NMR samples were made following the addition of 50 mM NaCl in order to minimise non-ideality effects (Monks et al., 1996). Sedimentation equilibrium distributions were formed by centrifugation at 40 000 rpm for 16–20 h at 20 °C and the absorbance profiles were measured using wavelengths from 230 to 290 nm. Data were analysed by nonlinear regression assuming a single species. A value of 0.72×10^{-3} m^3 kg^{-1}, as calculated from the amino acid composition, was used for the partial specific volume of these peptides. A value of 1.14×10^3 kg m^{-3} was used for the density of the 30% TFE-$^2H_3$/70% H_2O solution (MacPhee et al., 1997; Schuck et al., 1998).

Diffusion coefficient in water at 20 °C

In order to take into account the differences in temperature and viscosity among different solvents, it is convenient to convert the experimentally measured diffusion coefficients to standard conditions, usually water at 20 °C:

$$D_{20,w} = D_{obs}(293.2/T)(\eta_{T,w}/\eta_{20,w})(\eta_s/\eta_w) \quad (2)$$

where $D_{20,w}$ is the diffusion coefficient standardised to water at 20 °C, D_{obs} is the measured diffusion coefficient in the actual solvent at the experimental temperature, T, $\eta_{T,w}$ and $\eta_{20,w}$ are the viscosities of water at the temperature of the experiment (T) and at 20 °C, respectively, and η_s and η_w are, respectively, the viscosities of the solvent and water at a common temperature (Ralston, 1993).

Internal standard for diffusion measurements

In order to avoid the complications arising from variations of sample conditions, some small molecules have been used as internal viscosity standards (Chen et al., 1995; Jones et al., 1997). This internal viscosity standard may be considered as an internal radius standard if the effective hydrodynamic radius, $R_H^{Peptide}$, of the molecule is calculated

$$R_H^{Peptide} = R_H^{Ref} \times D_{Ref}/D_{Peptide} \quad (3)$$

This approach was employed in comparing native and urea-denatured lysozyme by PFGNMR diffusion measurements in order to avoid the complexities arising from variations in solution viscosity and temperature (Jones et al., 1997). Similarly, a change in the state of self-association may also alter its effective hydrodynamic radius.

Calculation of apparent molecular mass from translational diffusion coefficient

The relationship between molecular mass (M) and diffusion coefficient (D) is given by

$$M = (kT/6\pi\eta FD)^3[4\pi N_A/[3(\nu_2 + \delta_1\nu_1)]] \quad (4)$$

where k is the Boltzmann constant, T is the absolute temperature, η is the viscosity of the solution, N_A is Avogadro's number, ν_2 and ν_1 are the partial specific volumes of the molecule and solvent water, respectively, and δ_1 is the fractional amount of water bound to the molecule (hydration number) (Cantor and Schimmel, 1980). F is the shape factor, or Perrin factor, which is defined to be the ratio of the friction coefficient of the molecule (f) to that of a hard sphere (f_0) with equivalent mass and partial specific volume. For protein shapes modelled as rotational ellipsoids, F can be expressed in terms of the axial ratio p ($p = b/a$, with b being the equatorial radius and a being the semi-axis of revolution), as follows:
For a prolate ellipsoid ($p < 1$)

$$F = f/f_0 \quad (5a)$$
$$= (1-p^2)^{1/2}/(p^{2/3}\ln\{[1+(1-p^2)^{1/2}]/p\})$$

For an oblate ellipsoid ($p > 1$)

$$F = f/f_0$$
$$= (p^2-1)^{1/2}/\{p^{2/3}\tan^{-1}[(p^2-1)^{1/2}]\} \quad (5b)$$

Clearly, calculation of molecular mass, M, from the translational diffusion coefficient, D, using Equation 4 requires the values for η, ν_2, δ_1 and F to be known. In the present study, the viscosity of water at 20 °C, 1.002×10^{-3} N s m^{-2} (Weast, 1984), was used for the 10% ^2H_2O/90% H_2O solution. The viscosity for 30% TFE-$^2H_3$/70% H_2O was obtained from the original data of Schuck et al. (1998) to be 1.606×10^{-3} N s m^{-2}. The original data were fitted to a fourth-order polynomial with the constraint $\eta = 1.000$ when $x = 0$. The following relationship was obtained: $\eta = 1.000 + 2.133x + 1.670x^2 - 8.404x^3 + 4.948x^4$, where η donates the solution viscosity expressed relative to water and x donates the volume fraction of TFE per total volume of added TFE and water. A value of 0.72×10^{-3} m^3 kg^{-1} was used for the partial specific volume, as calculated from the amino acid composition (Perkins, 1986) without correction for the presence of TFE. Hydration numbers in the range 0.3–0.4 gram H_2O per gram of protein are common for most proteins. For highly charged short peptides like those in the current study, which probably have fewer 'buried' groups than proteins, the hydration number might be expected to be in the upper end of this range. Hydration values for these peptides calculated using values given by Kuntz and Kauzmann (1974) are 0.46–0.47. To allow for formation of the lactam bridge, the hydration of the charged Glu was replaced by that of Gln at position 28, reducing the hydration number to 0.41 (the hydration numbers for charged and uncharged Lys side chains are the same). A value of 0.4 was used for the hydration number, δ_1, in the present study. The overall dimensions of these peptides in water and aqueous TFE are similar, as shown in Figure 2. A value of 1.0325 was calculated for the shape-factor, F, by using Equation 5a for a prolate ellipsoid with an axial ratio of 0.55 for structures in both solvents.

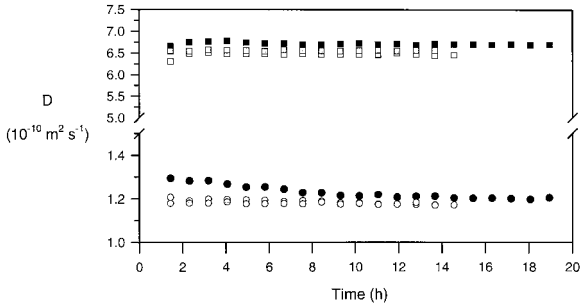

Figure 3. Summary of three sets of measured diffusion coefficients for NPY peptides (circles) and TFE (squares) in 30% TFE-$^2H_3$/70% H_2O. Black filled symbols: peptide **I** sample; grey filled symbols: peptide **II** sample; and open symbols: peptide **III** sample. The NMR probe temperature was equilibrated before the samples were introduced, and the acquisition of the first measurement started 1 h after the sample was inserted into the probe.

Results

Measurement of diffusion coefficients

To ensure that samples had equilibrated with respect to sample temperature and state of self-association, measurements were taken consecutively until no systematic change in the diffusion coefficients was observed. Figure 3 shows experimentally measured diffusion coefficients of NPY peptides in 30% TFE-$^2H_3$/70% H_2O versus time. Diffusion coefficients for TFE are also shown. A time-dependent decay is evident for peptide **I**, but not for the other two peptides. Slight differences in the diffusion coefficients of TFE across the three samples may result from minor variations in the volumetric fraction of TFE or the sample concentration.

Figure 4A shows that the precision of the measurements is very high. The two sets of data for peptide **II** in 30% TFE-$^2H_3$/70% H_2O were recorded several days apart with different maximum strengths of diffusion encoding gradients, favouring relatively faster diffusing species (TFE) and relatively slower diffusing species (the peptide), respectively. Figure 4B shows the diffusion coefficients for peptide **III** in H_2O/^2H_2O

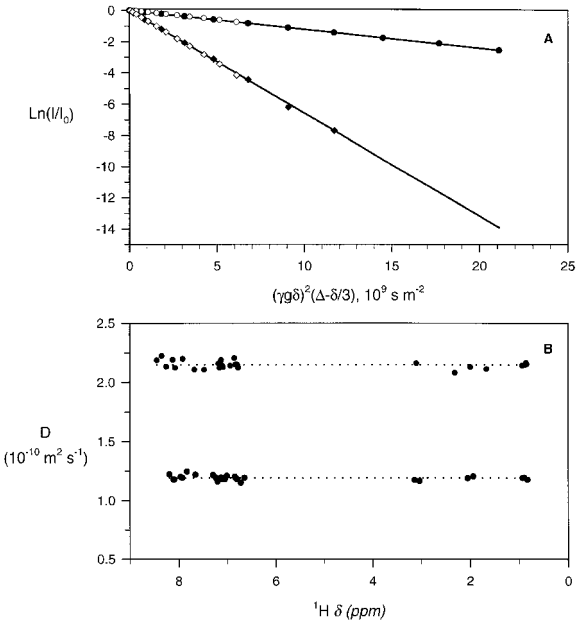

Figure 4. (A) Logarithmic (normalised) intensities of peptide **II** (●) and dioxane (♦) versus the strength of diffusion encoding, $\gamma^2 g^2 \delta^2(\Delta - \delta/3)$, from two independent measurements. Measurements were taken several days apart with different maximum strength of diffusion encoding to favour relatively faster diffusing species (TFE, open symbol) and slower diffusing species (peptide **II**, closed symbol), respectively. Lines represent the results of nonlinear regression to Equation 1 for the second data set. (B) Diffusion coefficients of peptide **III** in $H_2O/^2H_2O$, D = (2.15±0.03) × 10^{-10} m^2 s^{-1}, and in TFE-$^2H_3/H_2O$, D = (1.19±0.02) × 10^{-10} m^2 s^{-1}, obtained by fitting peak intensities to Equation 1 for most well-resolved peaks across the spectra.

and TFE-$^2H_3/H_2O$ obtained by fitting the peak intensities of different resonances across the spectrum to Equation 1. Peaks with different linewidths and intensities all give the same values, indicating excellent internal consistency for a given peptide under these conditions.

Effects of peptide concentration

In order to examine the effects of sample concentration on molecular diffusion coefficients, measurements were carried out at several concentrations for two peptides. Figure 5 plots the experimentally measured diffusion coefficients versus concentration for peptides **II** and **III** in both water and aqueous TFE. Only marginal changes were evident in the diffusion coefficients of these peptides at lower concentration in either solvent, indicating that, over this solute concentration range, viscosity changes were not significant and there was no dissociation of the peptide dimer (see below) in aqueous TFE. The following

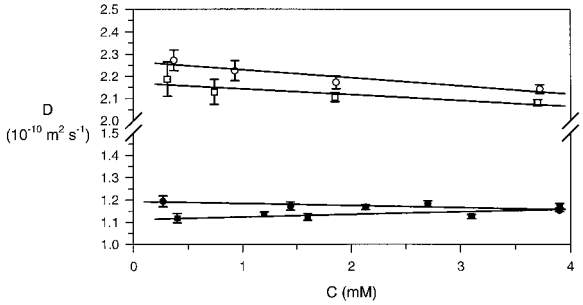

Figure 5. Experimentally measured diffusion coefficients for peptides **II** (squares) and **III** (circles) in both $H_2O/^2H_2O$ and TFE-$^2H_3/H_2O$ as a function of peptide concentration (expressed as the monomeric molar concentration) and their straight line fits. Values are the averages over a group of peaks across the spectrum for two separate measurements, with error bars representing the standard deviation.

relationships between peptide concentration (c) and diffusion coefficient (D) were obtained after fitting the data to a straight line (Lapham et al., 1997): in 10% ^2H_2O/90% H_2O, $D = 2.170 - 0.026\,c$ (peptide **II**) and $D = 2.266 - 0.036\,c$ (peptide **III**), and in 30% TFE-$^2H_3$/70% H_2O, $D = 1.112 + 0.012\,c$ (peptide **II**) and $D = 1.193 - 0.009\,c$ (peptide **II**). The slight increase in D at low peptide concentrations in water is consistent with the expectation that lower solute concentration would favour greater translational mobility, but it must be emphasised that the effect is small. In 30% TFE the concentration dependence is even less than in water, averaging to nearly zero over the two peptides.

Acetone, acetonitrile, dimethylsulfoxide and dioxane as internal viscosity standards

The ratios of the measured diffusion coefficients in water to those in aqueous TFE for these four low molecular weight solutes are plotted in Figure 6 as a function of the volumetric fraction of trifluoroethanol in TFE/H_2O mixture. Deviations among these potential internal standards are clearly evident. Also plotted in Figure 6 is the dependence of measured viscosity on TFE content, taken from Schuck et al. (1998). In general, all four solutes diffuse more slowly in aqueous TFE than predicted by the independent viscosity measurements, indicating that their diffusion behaviour is influenced by factors other than the macroscopic viscosity. Nevertheless, at low TFE concentrations the diffusion coefficient of acetonitrile matches the viscosity very well, and at higher TFE concentrations it remains the best choice, even though it deviates slightly from the viscosity curve. At these higher con-

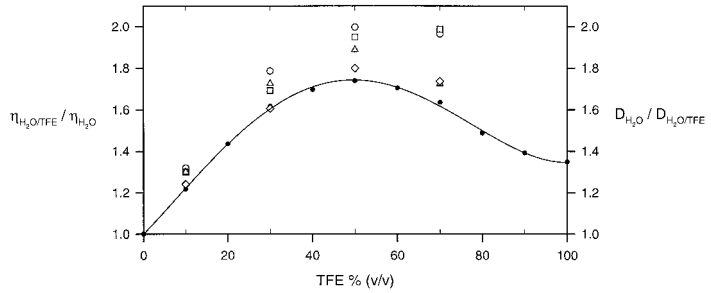

Figure 6. Plots of experimentally measured ratios of D_{H_2O}: D_{TFE/H_2O} (right axis) at different volumetric fraction of trifluoroethanol in TFE/H_2O mixture for dioxane (○), acetone (Δ), acetonitrile (◊) and dimethylsulfoxide (□). Previously published viscosities as a function of TFE content (relative to water, left axis) at 20 °C are shown as filled dots, with the line representing its best fit to the fourth-order polynomial equation (Schuck et al., 1998; see also Materials and methods).

centrations dimethylsulfoxide and dioxane are quite poor monitors of macroscopic viscosity.

Assessment of NPY peptide self-association

Experimentally measured diffusion coefficients and their corresponding values after corrections for the peptide concentration and solvent viscosity are summarised in Table 1 for peptides **I**–**III** in water and 30% TFE at 20 °C and pH 5.0. Apparent molecular masses for the peptides, calculated from translational diffusion coefficients using Equation 4, are compared with values obtained from sedimentation equilibrium analyses in Table 2. The apparent mass obtained by analytical ultracentrifugation for peptide **III** in water, 1340 (Table 2), is significantly lower than the expected mass of 1699. This sample contained 50 mM NaCl in an attempt to minimise non-ideality effects associated with the high positive charge of these peptides at pH 5 (Monks et al., 1996), but it seems that this did not eliminate the effect. At a peptide concentration of 0.37 mM (1/10 that used for the data in Table 2), an apparent mass of 1610 was obtained, which is in excellent agreement with the theoretical value and confirms the contribution of non-ideality at the higher concentration. A higher salt concentration was less effective at countering these effects, with an apparent mass of 1370 obtained at 3.7 mM peptide concentration and 150 mM NaCl. Based on our unpublished results on related peptides in aqueous TFE, we expect the effects of non-ideality to be less pronounced in this solvent. Thus, the apparent masses for peptides **I** and **III** are consistent with dimer formation, although the presence of a small fraction of trimer or tetramer cannot be ruled out. In the absence of TFE the peptides are monomeric. The apparent masses calculated from translational diffusion coefficients also show a substantial increase for all peptides in aqueous TFE in comparison with those in water, in good agreement with the ultracentrifugation results.

Discussion

Diffusion measurements are being used increasingly to monitor self-association phenomena and conformational changes in proteins. In this study we have investigated whether this approach is also applicable to peptides in the presence of trifluoroethanol, a commonly used co-solvent in structural studies of peptides. Defining the state of self-association of peptides under identical solution conditions to those used for the acquisition of NMR data to be used in structure calculations is particularly important in the case of peptides, where the number of long-range interactions is small (and in monomeric helical peptides usually zero). An incorrect assignment of long-range NOEs to intramolecular interactions, when in fact they arise partly or wholly from intermolecular interactions in an oligomeric state of the peptide, has the potential to produce incorrect structures. A good example of the importance of recognising self-association prior to structure calculations is provided by NPY itself, which clearly forms a dimer under the solution conditions used for NMR structure determination (Cowley et al., 1992; Monks et al., 1996). Assignment of the long-range NOEs observed under these conditions to intramolecular interactions would suggest that NPY adopts a hairpin fold. This structure may exist under other solution conditions (Nordmann et al., 1999), and even in the form bound to certain NPY receptor subtypes, but it is clearly not significantly populated under the conditions used for the structure determination.

The addition of trifluoroethanol to aqueous solutions of peptides is often used to stabilise helical

Table 1. Diffusion coefficients of peptides **I–III** in 10% ^2H_2O/90% H_2O and 30% TFE-$^2H_3$/70% H_2O at 20 °C and pH 5.0

	In 10% ^2H_2O/90% H_2O				In 30% TFE-$^2H_3$/70% H_2O			
	C[a] (mM)	D[b] (10^{-10} m^2/s)	D^{0} [c] (10^{-10} m^2/s)	$D^{0}_{20,w}$ [d] (10^{-10} m^2/s)	C[a] (mM)	D[b] (10^{-10} m^2/s)	D^{0} [c] (10^{-10} m^2/s)	$D^{0}_{20,w}$ [d] (10^{-10} m^2/s)
Peptide **I**	4.4	2.05 ± 0.01	2.19 ± 0.02	2.19 ± 0.02	2.7	1.23 ± 0.01	1.22 ± 0.01	1.95 ± 0.02
Peptide **II**	3.7	2.09 ± 0.01	2.20 ± 0.02	2.20 ± 0.02	3.9	1.18 ± 0.01	1.17 ± 0.01	1.87 ± 0.02
Peptide **III**	3.7	2.16 ± 0.02	2.27 ± 0.02	2.27 ± 0.02	2.7	1.19 ± 0.01	1.18 ± 0.01	1.89 ± 0.02

[a]Monomeric molar concentration of peptide, calculated from the sample weight.
[b]Diffusion coefficient measured at given sample concentration and experimental conditions.
[c]Extrapolated diffusion coefficients at 'zero concentration'. The following relationships were used: $D = D^0 - 0.031\,c$ (in H_2O) and $D = D^0 + 0.002\,c$ (in aqueous TFE); these were obtained by averaging the experimentally determined concentration dependencies of peptides **II** and **III** in each solvent (Figure 5).
[d]Diffusion coefficient at 'zero concentration' and expressed in terms of the standard solvent of water at 20 °C. A value of 1.002×10^{-3} N s m^{-2} (water) was assumed for the viscosity of the sample in 10% ^2H_2O/90% H_2O, and 1.606×10^{-3} N s m^{-2} for the viscosity of 30% TFE-$^2H_3$/H_2O at 20 °C (Schuck et al., 1998, see also Materials and methods).

structure (Nelson and Kallenbach, 1986; Sönnichsen et al., 1992). It is generally assumed that the resulting helical peptides are monomeric, but several recent studies show that this is not necessarily the case (Barden, 1995; Mulhern et al., 1995; MacPhee et al., 1997; Barnham et al., 1999) and it is also not true for the peptides investigated here. Thus, a reliable means of detecting self-association in peptides in water and TFE/water mixtures is important for structural studies in these solvents.

The results presented in this paper show that the diffusion measurements are very reproducible and that consistent values are obtained from different resonances in a given peptide. The concentration dependencies of the diffusion coefficient itself for two of the peptides in water and aqueous TFE were minor. Somewhat surprisingly, the diffusion coefficient for peptide **I** in aqueous TFE showed a significant time dependence, with a constant value being reached only after 10 h at 20 °C. This implies that its dimerisation in this solvent (see below) is very slow, and suggests that time dependencies should be assessed when accurate diffusion coefficients are sought. Peptides **II** and **III** showed no such time dependencies, even though peptide **II** differs from peptide **I** only in a Leu to Ile substitution at position 31.

The measured diffusion coefficients for the three peptides are similar to one another in the same solvent, although there are significant differences between their values in water and aqueous TFE (Table 1). After corrections for peptide concentration and solution viscosity, the diffusion coefficients expressed in terms of standard conditions (water at 20 °C) show a clear decline of about 16% for all peptides in aqueous TFE compared with water. This is smaller than the decrease of about 25% expected upon dimerization in an ideal case (Teller et al., 1979; Altieri et al., 1995), but is sufficient to permit the presence of self-association to be recognised.

Dioxane was used as an internal radius standard in a study of native and urea-denatured lysozyme by PFGNMR diffusion measurements in order to avoid the complexities arising from variations in solution viscosity and temperature (Jones et al., 1997). Several small organic molecules, acetone, acetonitrile, dimethylsulfoxide and dioxane, were evaluated in the present study as monitors of the solution viscosity upon addition of TFE. Although none of them fitted the independently measured macroscopic viscosity data of Schuck et al. (1998) perfectly, acetonitrile was clearly the best, and appears to be reliable at TFE concentrations up to about 40% by volume. One limitation of acetonitrile is that its methyl resonance is close to those of acetate and methionine, and in the present case, a reliable measurement of its diffusion coefficient was not obtained due to overlap with the resonance of the N-terminal acetyl group from the peptides. An increase of about 13% in the hydrodynamic radius of peptide **III** relative to DMSO was found in aqueous TFE compared with water, whereas increases of only 7% were observed relative to dioxane and acetone.

Another way of detecting molecular self-association is to calculate the apparent molecular mass from their diffusion coefficients. The calculated molecular masses showed substantial increases in aqueous TFE compared with water (Table 2). This was consistent with the results from sedimentation equilibrium

Table 2. Masses of C-terminal NPY analogues calculated from PFGNMR measurements of molecular self-diffusion and sedimentation equilibrium data in 10% ^2H_2O/90% H_2O and 30% TFE-$^2H_3$/70% H_2O at 20 °C and pH 5.0

	In 10% ^2H_2O/90% H_2O			In 30% TFE-$^2H_3$/70% H_2O		
	MW^a_{NMR}	MW^b_{NMR}	MW^c_{SE}	MW^a_{NMR}	MW^b_{NMR}	MW^c_{SE}
Peptide **I** (1770)[d]	2330	1911	–	2620	2685	3300
Peptide **II** (1770)[d]	2199	1886	–	2968	3044	–
Peptide **III** (1699)[d]	1992	1716	1340[e]	2893	2968	3700

[a]Apparent molecular mass calculated using Equation 4 from diffusion coefficients measured by PFGNMR (Table 1). Values for all other physical quantities used in the calculation are given in the text.
[b]Mass obtained using extrapolated diffusion coefficients at 'zero concentration'.
[c]Apparent molecular mass calculated using values from sedimentation equilibrium runs.
[d]Monomer mass calculated from the amino acid composition.
[e]A duplicate experiment gave a value of 1270, confirming that the experimental error is small. At one tenth this peptide concentration, i.e. 0.37 mM, a value of 1610 was obtained, while at 3.7 mM, increasing the NaCl concentration to 150 mM gave 1370.

analyses and implies significant self-association in aqueous TFE. Despite this general agreement, discrepancies were evident between the masses calculated from diffusion constants and those from sedimentation equilibrium, as well as with the theoretical values for monomer and dimer (Table 2). The apparent masses of the peptides in water are 18–32% larger than their theoretical monomeric values without correction for the effects of sample concentration, but in much better agreement after extrapolation of the diffusion coefficients to 'zero concentration'. On the other hand, as only marginal changes were observed as a function of concentration in TFE-$^2H_3$/H_2O, only very minor improvements were obtained when diffusion coefficients in this solvent were extrapolated to 'zero concentration'.

As can be seen from Equation 4, M is proportional to the inverse cube of the diffusion coefficient (D), viscosity (η), shape-factor (F) and temperature (T). Minor errors or uncertainties associated with D, η and F could therefore result in a significant error in the apparent mass. A calibration error of up to 2% in the strength of B_0 field gradient has been noted previously (Doran and Décorps, 1995), which will lead to a 4% error in the diffusion coefficient and eventually a 12% error in the mass calculation. In the present study, considerable attention was paid to calibration of the B_0 field gradient strength and a systematic offset was not evident in the calculated masses (Table 2), so errors in the calculated masses arising from uncertainties in the diffusion coefficient, D, are likely to be less significant than those from the viscosity, η, or the shape-factor, F. The value for the solvents viscosity is probably the major potential source of error. For example, using the viscosity of H_2O as an approximation for that of H_2O/^2H_2O mixture is likely to slightly undervalue this parameter, since ^2H_2O is more viscous than H_2O (Natarajan, 1989). In addition, the value of 1.606×10^{-3} N s m^{-2} for the viscosity of 30% TFE-^2H_2O/70% H_2O used in the present study may be slightly overvalued, which could explain why the calculated masses for these peptides in TFE/water were less than the theoretical values for dimers.

The shape-factor, F, represents another source of uncertainty. In aqueous TFE this was estimated from the NMR structure of the monomeric peptide unit, whereas the sedimentation equilibrium results clearly suggest that the peptides exist as dimers in this solvent. This shape-factor can vary significantly depending on the details of dimer formation. Figure 7 shows the theoretical ratio F_{dimer}:$F_{monomer}$ using a prolate ellipsoid model and two extreme models of dimer formation (see Equation 5a). It is clear that the actual F value for a dimer might take any value between the solid line, representing a 'side-by-side' dimer and the dotted line, representing an 'end-to-end' dimer. The peptides investigated here are more likely to resemble 'side-by-side' dimers, as in full length NPY (Monks et al., 1996). This type of dimerisation of monomers with an axial ratio of 0.55 will lead to a structure better modelled as an oblate rather than a prolate ellipsoid, with $p = 1.91$ and $F = 1.036$. This value for F is actually very close to that used in the present calculation, as estimated from the structure of a single unit. This implies that uncertainty in the shape-factor, F, is unlikely to be a major source of error in the masses

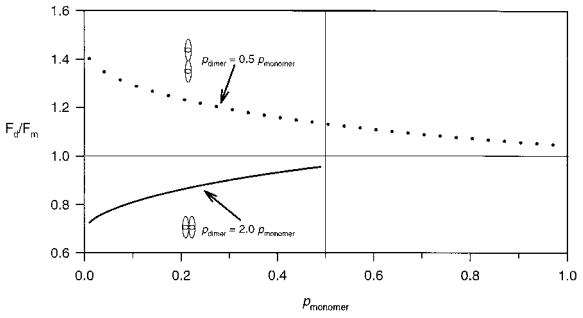

Figure 7. Plots of theoretical ratio of F_{dimer} and $F_{monomer}$ versus the axial ratio ($p = b/a$) of the monomer using prolate ellipsoid models for two ideal models of dimer formation. Dotted line: axial ratio of dimer half that of monomer. Solid line: axial ratio of dimer twice that of monomer (assuming the prolate ellipsoid model holds in both situations).

of these NPY peptides (Table 2). It is worth noting here that the sedimentation equilibrium results are not influenced by the molecular shape, as there is no net movement of the peptide once equilibrium is attained. Finally, we note that errors associated with the partial specific volume, ν, and peptide hydration number, δ_1, may also contribute to errors in the mass calculation; in the present study we have assumed the same values in water and aqueous TFE.

Conclusions

In conclusion, we have conducted translational self-diffusion coefficient measurements using PFGNMR for several peptide analogues of the C-terminus of NPY in both 10% ^2H_2O/90% H_2O and 30% TFE-^2H_2O/70% H_2O. Both direct comparison of translational diffusion coefficients after correction for solute concentration and solvent viscosity, and molecular masses calculated from their diffusion coefficients show that the peptides are mainly monomeric in water but associate to dimers in aqueous TFE. These results are consistent with those from sedimentation equilibrium experiments, which favour dimers over trimers as the predominant oligomeric state in this solvent. Quantitative determination of the self-association state of peptides from PFGNMR measurement of diffusion coefficients may be limited by experimental errors in the diffusion coefficient measurements and potential uncertainties associated with other parameters required in the calculation of molecular mass from the translational diffusion coefficient. Nevertheless, the calculated masses are sufficiently accurate to detect the presence of self-association, and for many peptides this will make diffusion measurements a very important adjunct to the suite of NMR experiments used to determine their solution structures.

Acknowledgements

We thank Mark Hinds, Kevin Barnham and Patrick McConville for helpful discussions. This research was supported in part by the Cooperative Research Centre for Biopharmaceutical Research.

References

Altieri, A.S., Hilton, D.P. and Byrd, R.A. (1995) *J. Am. Chem. Soc.*, **117**, 7566–7567.

Barden, J.A. (1995) *Biochem. Biophys. Res. Commun.*, **215**, 264–271.

Barden, J.A., Cuthbertson, R.M., Potter, E.K., Selbie, L.A. and Tseng, A. (1994) *Biochim. Biophys. Acta*, **1206**, 191–196.

Barnham, K.J., Catalfamo, F., Pallaghy, P.K., Howlett, G.J. and Norton, R.S. (1999) *Biochim. Biophys. Acta*, **1435**, 127–137.

Callaghan, P.T., Gros, M.A.L. and Pinder, D.N. (1983) *J. Chem. Phys.*, **79**, 6372–6381.

Cantor, C.R. and Schimmel, P.R. (1980) *Biophysical Chemistry, Part II: Techniques for the Study of Biological Structure and Function*, W.H. Freeman, New York, NY, pp. 539–590.

Chen, A., Johnson Jr., C.S., Lin, M. and Shapiro, M.J. (1998) *J. Am. Chem. Soc.*, **120**, 9094–9095.

Chen, A., Wu, D. and Johnson Jr., C.S. (1995) *J. Phys. Chem.*, **99**, 828–834.

Cowley, D.J., Hoflack, J.M., Pelton, J.T. and Saudek, V. (1992) *Eur. J. Biochem.*, **205**, 1099–1106.

Dingley, A.J., Mackay, J.P., Chapman, B.E., Morris, M.B., Kuchel, P.W., Hambly, B.D. and King, G.F. (1995) *J. Biomol. NMR*, **6**, 321–328.

Doran, S.J. and Décorps, M. (1995) *J. Magn. Reson.*, **A117**, 311–316.

Gibbs, S.J. and Johnson Jr., C.S. (1991) *J. Magn. Reson.*, **93**, 395–402.

Grundemar, L. (1997) In *Neuropeptide Y and Drug Development* (Grundemar, L. and Bloom, S.R, Eds.), Academic Press, San Diego, CA, pp. 1–11.

Grundemar, L. and Håkanson, R. (1994) *Trends Pharm. Sci.*, **15**, 153–158.

Houston, M.E., Gannon, C.L., Kay, C.M. and Hodges, R.S. (1995) *J. Pept. Sci.*, **1**, 274–282.

Jones, J.A., Wilkins, D.K., Smith, L.J. and Dobson, C.M. (1997) *J. Biomol. NMR*, **10**, 199–203.

Kirby, D.A., Britton, K.T., Aubert, M.L. and Rivier, J.E. (1997) *J. Med. Chem.*, **40**, 210–215.

Kuntz Jr., I.D. and Kauzmann, W. (1974) In *Advances in Protein Chemistry*, Vol. 28 (Anfinsen, C.B., Edsall, J.T. and Richards, F.M., Eds.), Academic Press, New York, NY, pp. 239–345.

Lapham, J., Rife, J.P., Moore, P.B. and Crothers, D.M. (1997) *J. Biomol. NMR*, **10**, 255–262.

Lin, M., Shapiro, M.J. and Wareing, J.R. (1997) *J. Am. Chem. Soc.*, **119**, 5249–5250.

Longsworth, L.G. (1960) *J. Phys. Chem.*, **64**, 1914–1917.

MacPhee, C.E., Perugrini, M.A., Sawyer, W.H. and Howlett, G.J. (1997) *FEBS Lett.*, **416**, 265–268.
Monks, S.A., Karagianis, G., Howlett, G.J. and Norton, R.S. (1996) *J. Biomol. NMR*, **8**, 379–390.
Mulhern, T.D., Howlett, G.J., Reid, G.E., Simpson, R.J., McColl, D.J., Anders, R.F. and Norton, R.S. (1995) *Biochemistry*, **34**, 3479–3491.
Natarajan, G. (1989) *Data Book on the Viscosity of Liquids*, Hemisphere, New York, NY.
Nelson, J.W. and Kallenbach, N.R. (1986) *Proteins Struct. Funct. Genet.*, **1**, 211–217.
Nordmann, A., Blommers, M.J.J., Fretz, H., Arvinte, T. and Drake, A.F. (1999) *Eur. J. Biochem.*, **261**, 216–226.
Pan, H., Barany, G. and Woodward, C. (1997) *Protein Sci.*, **6**, 1985–1992.
Perkins, S.J. (1986) *Eur. J. Biochem.*, **157**, 169–180.
Potter, E.K., Barden, J.A., McCloskey, M.J.D., Selbie, L.A., Tseng, A., Herzog, H. and Shine, J. (1994) *Eur. J. Pharmacol.*, **267**, 253–262.
Ralston, G. (1993) *Introduction to Analytical Ultracentrifugation*, Beckman Instruments, Inc., CA.
Rist, B., Zerbe, O., Ingenhoven, N., Scapozza, L., Peers, C., Vaughan, P.F.T., McDonald, R.L., Wieland, H.A. and Beck-Sickinger, A.G. (1996) *FEBS Lett.*, **394**, 169–173.
Schuck, P., MacPhee, C.E. and Howlett, G.J. (1998) *Biophys. J.*, **74**, 466–474.
Sönnichsen, F.D., Van Eyk, J.E., Hodges, R.S. and Sykes, B.D. (1992) *Biochemistry*, **31**, 8790–8798.
Stejskal, E.O. and Tanner, J.E. (1965) *J. Chem. Phys.*, **42**, 288–292.
Teller, D.C., Swanson, E. and de Haën, C. (1979) *Methods Enzymol.*, **61**, 103–124.
Weast, R.C. (1984) *CRC Handbook of Chemistry and Physics*, 64th ed., CRC Press, Boca Raton, FL.